DC vs. AC nanogrid backbones for office dwelling with building-integrated PV in Belgium

Konstantinos Spiliotis
ESAT-ELECTA, KU Leuven
EnergyVille
Leuven, Belgium
konstantinos.spiliotis@kuleuven.be

Kris Baert
ESAT-ELECTA, KU Leuven
EnergyVille
Leuven, Belgium
kris.baert@kuleuven.be

Johan Driesen
ESAT-ELECTA, KU Leuven
EnergyVille
Leuven, Belgium
johan.driesen@kuleuven.be

Abstract—The increasing penetration of renewable energy sources (RES), battery energy storage systems (BESS), and other loads native to DC, raises the question if a DC backbone topology may be more suitable compared to the commonly used AC. A number of studies that focused on this question, demonstrate a wide range of results that depending on the application and external conditions simulated. In this work, simulated DC and AC topologies are tested in an office building located in Belgium using a modelling framework developed in Modelica. The building is assumed to have a large penetration of building-integrated photovoltaics (BIPV) and battery energy storage systems (BESS) and a wide range of key performance indicators (KPI) are used to quantify the comparison. The DC topologies demonstrate increased performance when the BIPV system produces large amounts of power. The performance gains may be further enhanced by sizing optimally the less efficiency system components.

Index Terms—Building-Integrated Photovoltaics (BIPV), Electrical configuration, Modelling, Modelica, Building energy simulation

I. INTRODUCTION

Due to climate change and the legislation to mitigate it, the penetration of renewable energy sources (RES), BESS and DC loads is constantly increasing [1]. As a consequence, there is rising interest in DC nanogrids in a variety of dwellings, residential and commercial alike. DC grids have been implemented into a number of data centers, resulting in significant energy savings [2]. In a large number of studies, the DC vs. AC dilemma is revisited and the comparison between DC and AC grid implementations is quantified; DC grids efficiency gains are estimated between 2 % and 19 % compared to the AC equivalents [3]. Yet in another study, it is recommended that DC grid architectures might be beneficial in the future but not at the present conditions [4].

In this study, an office building in EnergyVille campus 'Thor Park' in Genk, Belgium is considered. The building is assumed to have façade-integrated BIPV modules on its south, west and east sides. The sizing of the BIPV system is in accordance to the building's external dimensions. The meteorological input and electrical load data used in this study are measured in the actual office building in EnergyVille campus. In comparison to other studies, a larger variety of different KPI is used to quantify the comparison. In addition, in the context of zero-energy buildings, very high penetration of both RES and BESS alike is considered. In the next section, the methodology and the modelling assumptions are presented. Section III, provides detailed information on the simulation procedure, section IV presents the results of the study, which is concluded in section V.

II. METHODOLOGY

A. Nanogrid backbone topologies

There are three different nanogrid backbone topologies that are studied in this work. The main comparison is between DC and AC backbones, however, different voltage levels for the DC topologies are considered too. While office appliances such as computers and printers, LED lights and ventilation fans are native to low DC voltage, HVAC central units are native to higher DC voltage, very commonly 380V. In this work half of the load is assumed to be native to 48V DC and the other half, native to 380V DC. Table I provides an overview of the nanogrid components included for each of the studied topologies.

The studied backbone topologies are illustrated in Fig. 1 and they are the following:

- 48V DC
- 380V DC
- 230V/50Hz AC

TABLE I
POWER ELECTRONIC COMPONENTS PER TOPOLOGY

System Component	Topology		
	48V DC	*380V DC*	*AC*
BIPV	DC/DC conv.	DC/DC conv.	DC/AC inv.
Battery[a]	DC/DC conv.	DC/DC conv.	DC/AC inv.
Low-volt. load	-	DC/DC conv.	AC/DC rect.
High-volt. load	DC/DC conv.	-	AC/DC rect.
Utility grid[a]	DC/AC inv.	DC/AC inv.	-

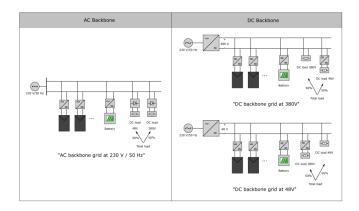[a]Bi-directional power electronic components.

Fig. 1. Nanogrid backbone topologies considered.

B. Modelling Framework

The models employed to perform the presented study are developed in Modelica. Modelica is an acausal, object-oriented modeling language ideal for multi-physics simulations [5]. Modelica has become popular in a wide range of applications due to its versatile, flexible and highly compatible nature. Modelica is currently used for modelling and simulations of building physics, heating and cooling equipment, electrical circuits and vehicle dynamics. The models used in this work originate in the openIDEAS library [6] and in previously published work [7], [8]. More details on the models used in this paper are given in the following subsections.
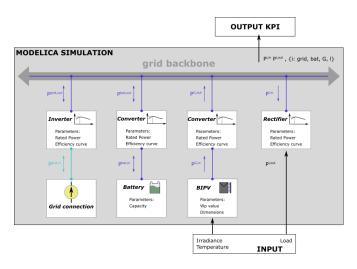

Fig. 2. Modelling framework at a glance. The building's nanogrid consists of BIPV modules, BESS, electrical loads, utility grid connection and of course the necessary power electronics to transform properly the voltages.

C. BIPV Module

The model of a façade-integrated BIPV module is implemented within the openIDEAS library and as part of a broader modelling framework developed for building energy simulations [7]. The model has been validated using an actual BIPV prototype installed in our in-house BIPV testing facility. The BIPV module consists of a stainless steel frame, a 60-cell

c-Si PV module of 244 Wp at STC[1] and a transparent, double glass glazing. The BIPV module contains also a cavity that allows natural, free-stream ventilation driven by the buoyancy force and the wind pressure. The model takes into account the radiative and convective heat transfer between the two sides of the cavity, the back of the the PV module and the building wall. The BIPV model estimates the energy generation as a function of the total irradiance on its plane and the PV cell temperature that is estimated internally.

D. Battery and Controller

In this work, the battery stack and management system (BMS) models given in the openIDEAS library are used [6]. The battery controller aims at maximizing the self-consumption within the building's nanogrid by charging the battery when there is a surplus between the BIPV-generated power and the electrical loads and discharging when there is deficit. It is possible to use the presented modelling framework to apply other strategies, such as minimizing energy costs with arbitrage however, these consideration are not in the scope of this paper.

E. Power Electronics

Finally, there is a number of power electronics modules needed to transform the voltage properly across the building's nanogrid. These modules include the module-level converters/inverters that connect the BIPV to the nanogrid backbone, bi-directional converter/inverter for the battery, rectifiers for the electrical loads and a bi-directional utility inverter. Unlike a large number of related works, in this paper the efficiency of the power electronic modules is variable and it is derived as a function of each module's loading factor with the use of its efficiency curve. The data on the efficiency curves are derived from a dedicated database of the Californian Utility Commission [9]. In this work, median curves for each of the considered grid components are used and as such, high specificity related to specific component curves is avoided. This approach is established in [3] and is adopted in this work.

III. SIMULATION

A. Input Data

Two periods have been studied in this work, 21-27 January 2018 and 22-28 July 2018. The input meteorological variables consisted of the ambient temperature T^{amb}, horizontal G^{horz} and diffuse irradiance G^{diff}, wind speed u^w and wind direction d^w and they have been measured at EnergyVille Building 1 in Thor Park, Genk, Belgium using the in-house meteorological station. The average values of the meteorological variables are given in Table II.

B. Key Performance Indicators

To substantiate a quantitative comparison between the different topologies considered in this work, a wide range of key performance indicators (KPI) is used. The selected KPI focus

---

[1]Standard Testing Conditions (STC): 25 °C, 1000 W/m^2

TABLE II
AVERAGE METEOROLOGICAL CONDITIONS FOR THE STUDIED PERIODS

Period	T^{amb} [°C]	G^{horz} [W/m²]	G^{diff} [W/m²]	u^w [m/s]	d^w [°]
21-27.01.2018	6.9	34.0	29.0	2.3	208
22-28.07.2018	25.7	242.7	107.3	1.5	174

on efficiency performance but also on system self-sufficiency and grid independence using KPI established in published work [10]. The total energy generation, E^G, generated within the office building is estimated as per Eq. 1. The generated power considered, P^G, is the power on the output of the BIPV-converter/inverter and therefore it differs across the different topologies tested. The system-level and component efficiencies are estimated according to Eq. 2-3 respectively. The system-level efficiency, η^σ, is the ratio of the sum of energy outputs over the sum of energy inputs to the system, e.g. the power flowing from BIPV to the converter is an input to the system and the power from the converter to the grid backbone is an output. The efficiency of component i is estimated as the ratio of output to input power through the component in question. The supply and demand cover factors are calculated as seen in Eq. 4-5. Supply cover factor, γ^s, is the ratio of energy consumed over the energy generated by BIPV during a period of time, here that is a week. The reverse relationship holds for the demand cover factor, γ^d. The load matching index, $\lambda(t)$, is a time-serie index expressing the ratio of generated power over the load, as seen in Eq. 6. Finally, the no-grid interaction probability, $p^{E\sim 0}$, in Eq. 7 captures the probability of zero power exchange (neither negative nor positive) between the building and the utility grid.

$$E^G = \int_T P^G(t)\,\mathrm{d}t \qquad (1)$$

$$\eta^\sigma = \frac{\sum_i E_i^{out}}{\sum_i E_i^{in}} \qquad (2)$$

$$\eta_i = \frac{P_i^{out}}{P_i^{in}} \qquad (3)$$

$$\gamma^s = \frac{\int_T min\{P^G(t) + P^{bat}(t), P^l(t)\}\,\mathrm{d}t}{\int_T P^G(t)\,\mathrm{d}t} \qquad (4)$$

$$\gamma^d = \frac{\int_T min\{P^G(t) + P^{bat}(t), P^l(t)\}\,\mathrm{d}t}{\int_T P^l(t)\,\mathrm{d}t} \qquad (5)$$

$$\lambda(t) = min\left\{1, \frac{P^G(t) + P^{bat}(t)}{P^l(t)}\right\} \qquad (6)$$

$$p^{E\sim 0} = \frac{t_{E^{net}=0} < 0.001}{\Delta t} \qquad (7)$$

IV. RESULTS AND DISCUSSION

The results of the simulations are summarized in Table III. During the assessed week in the winter, the performance of the AC topology is better. Specifically, the AC system's efficiency is higher by 11 % and 12 % than the 48V and the 380V DC systems respectively. On the other hand, more BIPV-generated power is eventually harvested in the DC topologies compared to the AC one due to the fact that DC/DC converters are on average more efficient than the DC/AC inverters. These gains over the AC topology are roughly 5 % for the 48V DC system and 2 % for the 380V one. Due to the low power generation at the BIPV system, the demand cover factor and load-matching index are negligible with no actual differentiation between the different topologies. On the other hand, during the week in the summer the DC systems perform better compared to the AC one. The 48V DC system provides an efficiency improvement of approximately 1 % compared to the AC system. The benefits of the DC systems are however highlighted by the other KPI; in the case of the 48V DC system, 81 % of the building's energy demand is covered by the BIPV generation. The median value of the load-matching index which incorporates concurrency to the demand cover factor is over 83 %, more than double compared to the AC system.

Evidently, integrating BIPV on EnergyVille Building 1 would help reduce the power flow from the grid. However, as the utility grid inverter is only partly loaded, it operates at lower efficiency as demonstrated in Fig. 3 where the component efficiencies for the 48V DC topology are given. As observed, the grid inverter operates with lower efficiency in the summer by approximately 10 % compared to the winter as it is partially loaded more frequently due to increased BIPV generation.

TABLE III
KEY PERFORMANCE INDICATORS SCORING PER TOPOLOGY

Topology	E^G [kWh]	η^σ [%]	γ^s [%]	γ^d [%]	$\overline{\lambda}(t)$[b] [%]	$p^{E\sim 0}$ [%]
			21-27 Janurary 2918			
48V DC	870.5	86.1	100.0	0.2	0.2	10
380V DC	845.6	85.9	100.0	0.2	0.2	9.5
AC	831.8	97.2	100.0	0.1	0.1	8.8
			22-28 July 2918			
48V DC	3148.0	96.9	100.0	81.3	83.3	41.9
380V DC	3053.0	96.1	100.0	52.6	53.2	39.5
AC	3003.0	96.2	100.0	40.6	41.0	35.4

[b]Median value of $\lambda(t)$.

V. CONCLUSIONS AND OUTLOOK

The simulated 48V DC topology demonstrates higher system efficiency than the AC topology during summer as the BIPV power generation is larger and there is less dependence on importing power from the utility grid. Reducing the losses in the utility grid inverter will improve significantly the performance of the 48V and 380V DC topologies in terms of system efficiency. Sizing optimally the grid inverter is key as its de-rating will limit the impact of partial loading. Regarding
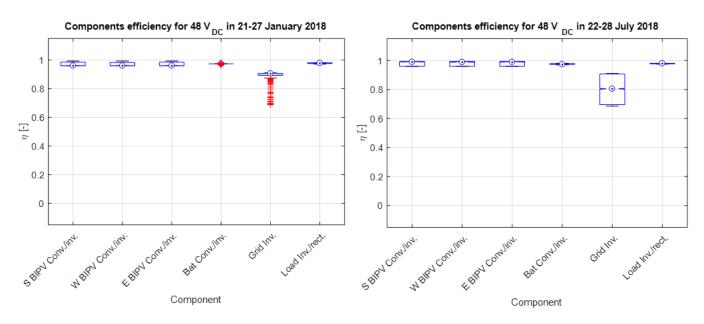
Fig. 3. Components efficiency for the 48V DC topology.

the demand cover factor, the load matching index and the no-grid interaction probability, the simulated DC topologies demonstrated better performance compared to the AC one. As a next step of this work, a detailed electricity consumption model for office buildings is being added. As such, the comparison between the simulated topologies might differ depending on the type of the loads and the climatic conditions. Finally, the sizing of the power electronic components will be optimized through parameter sweeping and therefore, the partial loading occurrences will not affect the comparison of the topologies.

VI. NOMENCLATURE

TABLE IV
TABLE OF ACRONYMS

Acronym	Explanation
BIPV	building-integrated photovoltaic(s)
RES	renewable energy sources
BESS	battery energy storage system(s)
HVAC	heating, ventilation and air cooling
STC	standard testing conditions
KPI	key performance indicator(s)

TABLE V
TABLE OF SYMBOLS

Symbol	Explanation
T^{amb}	ambient temperature
$G^{horz/diff}$	horizontal/diffuse irradiance
u^w	wind speed
d^w	wind direction
E^G	generated energy
P^G	generated power
η^σ	system efficiency
η_i	component i efficiency
γ^s/d	supply/demand cover factor
P^{bat}	power to/from BESS
P^l	active power load
$\lambda(t)$	load-matching index
$p^{E\sim0}$	no grid interaction probability
$t_{E_{net}=0}$	time with zero energy interaction

REFERENCES

[1] K. Spiliotis, A. I. Ramos Gutierrez, and R. Belmans, "Demand flexibility versus physical network expansions in distribution grids," *Applied Energy*, vol. 182, pp. 613–624, Nov. 2016.

[2] G. AlLee and W. Tschudi, "Edison Redux: 380 Vdc Brings Reliability and Efficiency to Sustainable Data Centers," *IEEE Power and Energy Magazine*, vol. 6, no. 10, pp. 50–59, 2012.

[3] D. L. Gerber, V. Vossos, W. Feng, C. Marnay, B. Nordman, and R. Brown, "A simulation-based efficiency comparison of AC and DC power distribution networks in commercial buildings," *Applied Energy*, vol. 210, pp. 1167–1187, Jan. 2018.

[4] F. Dastgeer and H. E. Gelani, "A Comparative analysis of system efficiency for AC and DC residential power distribution paradigms," *Energy and Buildings*, vol. 138, pp. 648–654, Mar. 2017.

[5] P. Fritzson, *Principles of Object-Oriented Modeling and Simulation with Modelica 2.1*. John Wiley & Sons, Aug. 2010. Google-Books-ID: doNqLi7279wC.

[6] F. Jorissen, G. Reynders, R. Baetens, D. Picard, D. Saelens, and L. Helsen, "Implementation and verification of the IDEAS building energy simulation library," *Journal of Building Performance Simulation*, vol. 0, pp. 1–20, Feb. 2018.

[7] K. Spiliotis, J. Gonalves, C. Baert, J. Driesen, and D. Saelens, "From BIPV module to system: A modelica-developed framework for building

energy simulations including BIPVs," in *35th European PV Solar Energy Conference and Exhibition (EU PVSEC)*, (Brussels, Belgium), pp. 1619–1622, WIP; Munich, Germany, Nov. 2018.

[8] K. Spiliotis, J. E. Gonalves, W. Van De Sande, S. Ravyts, M. Daenen, D. Saelens, K. Baert, and J. Driesen, "Modeling and validation of a DC/DC power converter for building energy simulations: Application to BIPV systems," *Applied Energy*, vol. 240, pp. 646–665, Apr. 2019.

[9] California Public Utilities Commission, "Inverter Performance Test Summaries," 2016.

[10] R. Baetens, R. De Coninck, J. Van Roy, B. Verbruggen, J. Driesen, L. Helsen, and D. Saelens, "Assessing electrical bottlenecks at feeder level for residential net zero-energy buildings by integrated system simulation," *Applied Energy*, vol. 96, pp. 74–83, Aug. 2012.